Manganese and Calcium Requirements for Reconstitution of Oxygen-Evolution Activity in Manganese-Depleted Photosystem II Membranes†

Anne-Frances Miller‡ and Gary W. Brudvig*

Department of Chemistry, Yale University, New Haven, Connecticut 06511

Received December 14, 1988; Revised Manuscript Received May 22, 1989

ABSTRACT: The Mn complex of photosystem II and O_2-evolution activity are reconstituted in Mn-depleted photosystem II membranes in a light-dependent process called photoactivation. Recovery of O_2-evolution activity requires both Mn^{2+} and Ca^{2+} in the photoactivation medium. The Mn^{2+} and Ca^{2+} dependences of both the effective rate constant and yield of photoactivation have been determined. A comparison of these data with the predictions of mathematical models for photoactivation leads to the conclusion that photoactivation occurs in two stages. The first stage, photoligation of Mn, requires light and depends primarily on Mn^{2+}. The second stage, binding of Ca^{2+}, is required for expression of O_2-evolution activity. This two-stage model affords an excellent fit to the data and provides dissociation constants and binding stoichiometries for Ca^{2+} and Mn^{2+}. We conclude that one Mn^{2+} ion is bound and photooxidized in the rate-determining step(s) of photoactivation. On the basis of these results and data already in the literature, the molecular details of the elementary steps in photoactivation are discussed and a mechanism of photoactivation is proposed.

Photoactivation is the process by which the catalytic Mn complex of photosystem II is assembled from Mn^{2+} ions and O_2-evolution activity is acquired or restored. This reaction was first reported by Cheniae and Martin (1966) and Gerhardt and Weissner (1967) in Mn-deficient algae, and these observations were extended in a variety of samples ranging from Tris-treated chloroplasts to chloroplasts from wheat seedlings greened in intermittent light (Yamashita & Tomita, 1971; Ono & Inoue, 1982). The term photoactivation reflects the finding that assembly of the Mn complex is dependent on illumination of photosystem II (Cheniae & Martin, 1967), as well as Mn^{2+} (Eyster et al., 1958; Homan, 1967). Several studies also suggested that Ca^{2+} is required for photoactivation (Yamashita & Tomita, 1976; Ono & Inoue, 1983; Pistorius & Schmid, 1984).

Illumination is necessary for photoactivation, but can also result in photoinhibition, causing loss of primary photochemical activity. Photoinhibition has been proposed to result from oxidative damage to photosystem II, a consequence of the powerful oxidant generated upon light-induced charge separation (Thompson & Brudvig, 1988). Although the term photoinhibition is usually applied to the loss of photochemical activity that accumulates during intense illumination of O_2-evolving photosystem II (Jones & Kok, 1966), photosystem II membranes lacking O_2-evolution activity are photoinhibited by irradiation only $^1/_{50}$ as intense (Callahan et al., 1986).

Recently, photoactivation has been demonstrated in isolated photosystem II membranes treated with 5 mM NH_2OH to remove Mn (Tamura & Cheniae, 1986, 1987a). Whereas photosystem II centers damaged by photoinhibition can be repaired and eventually photoactivated in systems containing intact chloroplasts capable of protein synthesis (Callahan & Cheniae, 1985), photoinhibition is irreversible in isolated photosystem II membranes. Nonetheless, the advantage of studying isolated photosystem II membranes is that the observed rate of photoactivation does not include the rates of ion transport or repair-related processes that occur when photoinhibited centers are reactivated in chloroplasts (Callahan et al., 1986). The photoactivation process displays first-order kinetics (Tamura & Cheniae, 1987a), which can be uniquely described by an effective rate constant and the final yield of photoactivation. Both of these parameters reflect important underlying characteristics of photoactivation.

Both Mn^{2+} and Ca^{2+} stimulate photoactivation at low concentrations, but Mn^{2+} is inhibitory at higher concentrations. This inhibition can be counteracted by raising the Ca^{2+} concentration. Thus, Mn^{2+} and Ca^{2+} were each proposed to behave as competitive inhibitors at the other's binding site (Ono & Inoue, 1983; Tamura & Cheniae, 1986; 1987a). However, past studies of the effects of different metal ions on photoactivation (Ono & Inoue, 1983) have been done in intact chloroplasts and might be complicated by ion transport, competition from other Ca^{2+}-binding sites, and interfering Ca^{2+} effects.

Past reports of Mn^{2+} and Ca^{2+} requirements for photoactivation have failed to produce definite information as to the nature of the requirements or their relation to the mechanism of photoactivation. Also, the photoactivation reaction, in which one of the substrates is also the enzyme, does not lend itself to some of the assumptions used in the development of the common models for enzymatic reactions. Therefore, we have analyzed the Mn^{2+} and Ca^{2+} dependence of photoactivation in isolated photosystem II membranes, using models specifically designed to treat the photoactivation reaction. Comparison of our data with the predictions of the models has enabled us to ascertain the nature of the Mn^{2+} and Ca^{2+} requirements for photoactivation. We have also obtained dissociation constants and binding stoichiometries for Mn^{2+} and Ca^{2+} in the rate-determining steps of photoactivation that give new insight into the mechanism of photoactivation.

†This work was supported by the National Institutes of Health (GM32715). G.W.B. is the recipient of a Camille and Henry Dreyfus Teacher/Scholarship.

‡Present address: Department of Chemistry, Massachusetts Institute of Technology, Cambridge, MA 02139.

0006-2960/89/0428-8181$01.50/0

Table I: Effects of NH_2OH Treatment and Subsequent Photoactivation on O_2-Evolution Activity, S_2-State Multiline EPR Signal Intensity, and Mn Content of Photosystem II Membranes[a]

sample type	O_2-evolution activity [μmol of O_2/(mg of Chl·h)]	multiline EPR signal intensity (%)	Mn/200 Chl
Photoactivation in 5 mM Ca^{2+} and 60 μM Mn^{2+}			
untreated photosystem II membranes	560 (100%)	100	4.2 (100%)
NH_2OH-treated photosystem II membranes	≤12 (≤2%)	0	0.1 (2%)
photoactivated NH_2OH-treated photosystem II membranes	169 (30%)	30	1.4 (33%)
Photoactivation in 50 mM Ca^{2+} and 1 mM Mn^{2+}			
untreated photosystem II membranes	363 (100%)	100	4.0 (100%)
NH_2OH-treated photosystem II membranes	33 (9%)	11	0.3 (8%)
photoactivated NH_2OH-treated photosystem II membranes	147 (40%)	38	1.6 (40%)

[a] The yield of photoactivation is given as the O_2-evolution activity recovered after 40 min of photoactivation. This activity survived one wash in each of HSCa buffer with 1 mM EDTA and then HSCa buffer, performed to remove extraneous Mn^{2+}. Both the Mn content and S_2-state multiline EPR signal intensity were determined after washing.

Materials and Methods

Photosystem II membranes were prepared from market spinach as in Berthold et al. (1981) as modified by Beck et al. (1985), treated with 5 mM NH_2OH to remove Mn as in Tamura and Cheniae (1987a), in 0.4 M sucrose, 50 mM MES[1]/NaOH, pH 6.5, 15 mM NaCl, and 1 mM $CaCl_2$, and washed twice in 30% ethylene glycol, 25 mM MES, pH 6.5, and 10 mM NaCl. The photosystem II membrane preparations typically had O_2-evolution activities of 450 μmol of O_2/(mg of Chl·h) before treatment with NH_2OH and residual activities of up to 30 μmol of O_2/(mg of Chl·h) afterward. Five percent of the extrinsic 33-kDa polypeptide, 25% of the 23-kDa polypeptide, and 40% of the 17-kDa polypeptide were lost in the course of NH_2OH treatment, as estimated by sodium dodecyl sulfate–polyacrylamide gel electrophoresis and staining with Coomassie brilliant blue R-250, as in de Paula et al. (1986). Nonetheless, addition of an excess of the extrinsic polypeptides to the photoactivation medium did not discernibly alter the Mn^{2+} and Ca^{2+} dependence of photoactivation under the conditions used; this may be because the fraction of photosystem II centers that are photoactivated binds the extrinsic polypeptides more tightly than the others (Becker et al., 1985), and the maximum percent of photoactivated centers does not exceed the availability of the extrinsic polypeptides. Photosystem II membranes depleted in 17- and 23-kDa polypeptides were prepared by treatment with 2 M NaCl as in de Paula et al. (1986).

Photoactivation was conducted in 0.5-mL batches, in 10-mL beakers illuminated with incandescent bulbs (1 W/m^2 at the sample on the basis of bolometric measurement), at room temperature (approximately 22 °C). Because the rates of both photoactivation and photoinhibition depend on the intensity of illumination (Jones & Kok, 1966; Cheniae & Martin, 1971), the same illumination conditions were used throughout this work. The medium contained 50 mM MES/NaOH, pH 6.5, 12.5 μM DCIP, and 0.25 mg of Chl/mL, but the Mn^{2+} and Ca^{2+} concentrations were varied over a range from 6 μM to 20 mM $MnSO_4$ and from 0.5 to 50 mM $CaCl_2$, respectively. The Cl^- concentration was adjusted to 100 mM in all cases with NaCl. NH_2OH-treated photosystem II membranes at 5 mg of Chl/mL were added to the photoactivation medium, and the mixture was allowed to equilibrate at room temperature in the dark for 1–2 min before photoactivation was begun by transferring the sample into the light.

Photoactivation was monitored by O_2-evolution activity assays (Beck et al., 1985), in 5 mM $CaCl_2$, 10 mM NaCl, 20 mM MES/NaOH, pH 6.0, 1 mM $K_3Fe(CN)_6$, and 250 μM DCBQ. Inspite of the inclusion of Ca^{2+} in the O_2-evolution assays, the O_2-evolution rates accurately reflected the Ca^{2+} content of the photoactivation medium and did not include significant contributions from photosystem II centers that only bound Ca^{2+} after addition to the O_2-evolution assay. Samples photoactivated in the presence of low Ca^{2+} concentrations exhibited negligible O_2-evolution activity. The illumination period of the assays lasted less than 30 s, and the rate of O_2 evolution was constant after an initial delay of less than 5 s.

O_2-evolution activity assays were performed at 4-min intervals initially, and after 30 min, at which point the photoactivation reaction had reached completion (precision of ±5 s). The residual O_2-evolution activity of (unactivated) NH_2OH-treated photosystem II membranes was subtracted to give activities representing the extent of photoactivation. When the activity gains were large enough, they were analyzed in terms of first-order kinetics to give the effective rate constant and yield of photoactivation for each combination of Mn^{2+} and Ca^{2+} concentrations. All fitting of equations to data was performed with the nonlinear-fitting module of SYSTAT (version 3.1, 1987, SYSTAT Inc.).

For EPR studies, NH_2OH-treated photosystem II membranes were photoactivated in 6-in. Petri dishes to limit the path length of light in the photoactivation medium to 2 mm. The photosystem II membranes were collected after photoactivation for 0.5–1 h and washed once in high-salt Ca^{2+} (HSCa) buffer [200 mM NaCl, 15 mM $CaCl_2$, 25 mM MES/NaOH, pH 6.5, 30% (v/v) ethylene glycol] with 1 mM EDTA and then once in HSCa buffer alone, by centrifugation and resuspension to 0.5 mg of Chl/mL, to remove extraneous Mn^{2+}. Chl was assayed as in Arnon (1949), and Mn content per photosystem II center was assayed by EPR as in Babcock et al. (1983) and Yocum et al. (1981). The S_2-state multiline EPR signal was measured as described in Beck et al. (1985), and other EPR signals arising from photosystem II were quantitated as in de Paula et al. (1985).

Results

Depletion and Reconstitution of Manganese. Photoactivation leads to substantial recovery of the O_2-evolution activity that was abolished by treatment with NH_2OH, as shown in Table I. The recovered O_2-evolution activity did not decrease in the course of one wash in each of HSCa buffer with 1 mM EDTA and HSCa buffer alone. The extent of restoration of O_2-evolution activity upon photoactivation correlates well with

[1] Abbreviations: Chl, chlorophyll; D, tyrosine residue in photosystem II that gives rise to EPR signal II_{slow} when oxidized; DCBQ, 2,5-dichloro-*p*-benzoquinone; DCIP, 2,6-dichlorophenolindophenol; DCMU, 3-(3,4-dichlorophenyl)-1,1-dimethylurea; DPC, diphenylcarbazide; EDTA, ethylenediaminetetraacetic acid; EPR, electron paramagnetic resonance; kDa, kilodaltons; MES, 2-(*N*-morpholino)ethanesulfonic acid.

the magnitude of the S_2-state multiline EPR signal, and also with Mn content (Table I), as has been reported for photosystem II membranes treated in various ways [reviewed in Babcock (1987)]. This correlation indicates that the Mn bound in photoactivated photosystem II membranes represents four Mn ions bound functionally in 30 or 40% of the photosystem II centers, and a negligible population of photosystem II centers containing stably bound but inactive Mn.

Figure 1 compares the S_2-state multiline EPR signal produced in photoactivated NH_2OH-treated photosystem II membranes with the signal produced in untreated photosystem II membranes. Although the S_2-state multiline EPR signal from the photoactivated photosystem II membranes is only 40% as intense as the signal from untreated membranes, it is identical with the control signal. Thus, the structure of the reconstituted Mn complex appears to be identical with the structure prior to depletion and reconstitution of Mn, consistent with the correlation between recovery of O_2-evolution activity and four Mn per photosystem II center.

Quantitation and summation of the extent of photooxidation of all the electron donors, cytochrome b_{559}, Chl, D, and the Mn complex, confirmed that approximately one stable charge separation occurred in all photosystem II centers upon illumination at 215 K, in all three types of samples (shown in Figure 1). In NH_2OH-treated photosystem II membranes (Figure 1a), the charge-separation reaction produced predominantly oxidized cytochrome b_{559} (the g_y turning point is observed at approximately 3000 G) and reduced Q_A (Q_A^- interacting with Fe^{2+} has a turning point at approximately 3600 G), whereas in untreated photosystem II membranes (Figure 1c) the Mn complex is oxidized, giving the S_2-state multiline EPR signal, and Q_A is also reduced. In photoactivated photosystem II membranes (Figure 1b), both cytochrome b_{559} and the Mn complex are photooxidized in fractional yields representing centers that have not and have been photoactivated, respectively. Therefore, the smaller size of the S_2-state multiline EPR signal in photoactivated photosystem II membranes is not an artifact of inefficient charge stabilization, but a reflection of the fraction of photosystem II centers containing a native Mn complex.

Model for the Mn^{2+} and Ca^{2+} Dependence of Photoactivation. The Mn^{2+} and Ca^{2+} dependence of the yield of photoactivation is illustrated in Figure 2, which shows the final yield of photoactivation as a function of the Mn^{2+} concentration in the medium, in the presence of 0.5 or 50 mM Ca^{2+}. The yield of photoactivation increases with added Mn^{2+} at first, in 0.5 and 50 mM Ca^{2+}, but in both cases there is an optimum Mn^{2+} concentration above which Mn^{2+} is inhibitory. Figure 2 shows that above 100 μM Mn^{2+} 50 mM Ca^{2+} relieves the inhibition of photoactivation due to excessive Mn^{2+} and leads to higher O_2-evolution activity yields. High concentrations of Ca^{2+} may also compete with low concentrations of Mn^{2+} for the Mn-binding site because increasing the Ca^{2+} concentration from 0.5 to 50 mM Ca^{2+} appears to be inhibitory at Mn^{2+} concentrations below 6 μM, but any competition at the Mn-binding site is extremely weak. Thus, our data demonstrate competition between Mn^{2+} and Ca^{2+} for the Ca^{2+}-binding site, in agreement with Ono and Inoue (1983) and Tamura and Cheniae (1987a) and also provide evidence for competition between Ca^{2+} and Mn^{2+} for the Mn-binding site.

Both Mn^{2+} and Ca^{2+} are necessary for photoactivation. However, two different modes of participation have been advanced for Ca^{2+} in photoactivation. Ono and Inoue (1983) proposed that both Ca^{2+} and Mn^{2+} must be bound in their appropriate sites for assembly of the Mn complex and photoactivation to occur. In contrast, Tamura and Cheniae

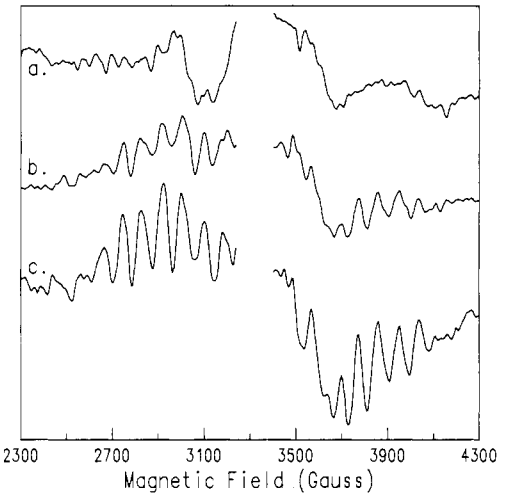

FIGURE 1: EPR signals produced by illumination at 215 K in photosystem II membranes depleted of Mn and reconstituted. The EPR spectra are illuminated-minus-dark difference spectra from (a) NH_2OH-treated photosystem II membranes, (b) NH_2OH-treated photosystem II membranes after photoactivation, and (c) untreated photosystem II membranes. The three spectra are shown scaled by the Chl concentrations of the samples. EPR conditions: microwave frequency, 9.1 GHz; temperature, 7 K; microwave power, 0.2 mW; field modulation amplitude, 20 G; field modulation frequency, 100 kHz.

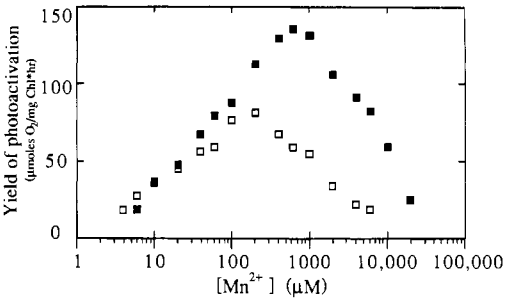

FIGURE 2: Comparison of the yield of photoactivation as a function of the Mn^{2+} concentration, at two different Ca^{2+} concentrations. The O_2-evolution activity recovered after 30 min of photoactivation (by which time the photoactivation was complete in all cases) is plotted against the Mn^{2+} concentration on a logarithmic scale. (■) 50 mM Ca^{2+}; (□) 0.5 mM Ca^{2+}. An average of two independent photoactivations was performed at each combination of Mn^{2+} and Ca^{2+} concentrations, and the average standard deviation in photoactivation yield was 7 μmol of O_2/(mg of Chl·h).

(1987b) report that photosystem II can photoligate four Mn without recovery of O_2-evolution activity in the absence of Ca^{2+} and then bind Ca^{2+} in the dark, acquiring O_2-evolution activity in the process. In the first case, photoactivation would occur in one stage dependent on both Mn^{2+} and Ca^{2+}. In the second case, photoactivation would proceed in two stages: Mn^{2+}-dependent Mn photoligation followed by Ca^{2+} binding. Although these two schemes predict similar Ca^{2+} and Mn^{2+} dependences for the yield of photoactivation, their predictions with respect to the rate of photoactivation differ sharply. To clarify these differences and choose the scheme that best describes photoactivation, the mathematical expressions for the predictions of the two schemes are developed below.

Before the photoactivation process is initiated by illumination, the sample contains unactivated photosystem II centers that lack a functional Mn complex. The unactivated photosystem II is assumed to bind Mn^{2+} and Ca^{2+} in rapid equilibrium with Mn^{2+} and Ca^{2+} in the bulk medium. On the basis of the data in Figure 2, Mn^{2+} and Ca^{2+} are both considered to compete for each of the Mn- and Ca^{2+}-binding sites. The sites are assumed to be independent of one another so that the

dissociation constants for each metal ion at one site can be assumed not to depend on the content of the other site. The dissociation constants are defined as follows for binding of Ca^{2+} in the Ca^{2+}-binding site

$$K_{Ca} = \frac{[Ca^{2+}]^y[P]}{[Ca_yP]} = \frac{[Ca^{2+}]^y[PMn_z]}{[Ca_yPMn_z]} = \frac{[Ca^{2+}]^y[PCa_b]}{[Ca_yPCa_b]} \quad (1)$$

where P is an unactivated photosystem II center with the Ca^{2+}-binding site content indicated on the left and the Mn-binding site content on the right, y is the binding stoichiometry of Ca^{2+} in the Ca^{2+}-binding site, and b and z are the binding stoichiometries of Ca^{2+} and Mn^{2+}, respectively, in the Mn-binding site. Similarly, K_{Mn} is the dissociation constant for Mn^{2+} at the Mn-binding site, K'_{Ca} and K'_{Mn} are the dissociation constants for Ca^{2+} and Mn^{2+}, respectively, in the other's binding site, and a is the binding stoichiometry for Mn^{2+} in the Ca^{2+}-binding site. Equilibrium binding at each of the Ca^{2+}- and Mn-binding sites results in an equilibrium among different forms of unactivated photosystem II centers characterized by different Ca^{2+}- and Mn-binding site contents.

During illumination under appropriate conditions, those photosystem II centers with the correct ion(s) bound can photoligate Mn. Mn photoligation is an irreversible process on the time scale of the photoactivation. Consequently, those centers that successfully photoligate Mn are removed from the equilibrium among unactivated photosystem II centers. Eventually, all of the unactivated photosystem II centers would be expected to succeed in photoligating Mn. However, conditions producing low rates of photoactivation also produced low yields, even when extra time was allowed to compensate for the low rate of photoactivation. Therefore, photoactivation must occur in parallel with an inactivating photochemical process that reduces the yield of photoactivation by competing with it for the pool of unactivated photosystem II centers. We have called this process photoinactivation.

These considerations lead to the following picture of photoactivation. The initial unactivated photosystem II centers bind either Mn^{2+} or Ca^{2+} at the Mn- and Ca^{2+}-binding sites. Some fraction of these centers contain an ion complement that enables them to successfully photoligate Mn, and the concentration of such competent centers depends on the ambient Mn^{2+} and Ca^{2+} concentrations. Upon illumination, photoactivation and photoinactivation consume the pool of unactivated photosystem II, at rates proportional to the populations of photosystem II susceptible to each. Thus, the population of unactivated photosystem II should decrease exponentially with an effective rate constant of

$$\kappa = k_i + (k_l/K_A) \quad (2)$$

where k_i and k_l are the rate constants of photoinactivation and Mn photoligation, respectively, and K_A is the ratio of the total population of unactivated photosystem II, all assumed to be susceptible to photoinactivation, to the population of unactivated photosystem II with the correct metal ions bound for Mn photoligation.

In our experiments, we have monitored the time course of photoactivation by withdrawing aliquots from the reaction mixture and immediately measuring their O_2-evolution activity. In order for a photosystem II center to evolve O_2, it must have photoligated Mn. We denote photosystem II centers with a functional Mn complex assembled by PSII. However, Ca^{2+} must also be bound before O_2 evolution can occur. Thus, only centers with the Mn complex assembled and Ca^{2+} bound are detected by our assay. We denote these centers by CaPSII. The final O_2-evolution activity yield of photoactivation is a measure of the yield of CaPSII

$$\text{final yield of photoactivation} \propto [\text{CaPSII}]_{t=\infty} \quad (3)$$

where $t = \infty$ denotes the time at which photoactivation is complete and the maximum yield of O_2 evolution is attained.

Whether Ca^{2+} must be bound prior to photoligation of Mn or binds rapidly afterward, the population of photosystem II with the Mn complex assembled and Ca^{2+} bound is predicted to increase with photoactivation time as

$$[\text{CaPSII}] = [\text{CaPSII}]_{t=\infty}(1 - e^{-\kappa t}) \quad (4a)$$

$$[\text{CaPSII}]_{t=\infty} = k_l[P_{TOT}]_{t=0}/\kappa K_1 K_2 \quad (4b)$$

where [CaPSII] denotes the population with the Mn complex assembled and Ca^{2+} bound at time t in the photoactivation, $[P_{TOT}]_{t=0}$ is the inital population of unactivated photosystem II, and K_1 and K_2 are equilibrium constants relating the total population of photosystem II centers to the populations with the correct ion bound in the Mn- and Ca^{2+}-binding sites, respectively. If Ca^{2+} need not be bound prior to Mn photoligation, then the effective rate constant of Mn photoligation depends only on the ratio of all unactivated photosystem II centers to those with Mn^{2+} bound in the Mn-binding site, $K_A = K_1$, and

$$\kappa = k_i + (k_l/K_1) \quad (5)$$

K_1 can be written in terms of the dissociation constants for Mn^{2+} and Ca^{2+} at the Mn-binding site and the Mn^{2+} and Ca^{2+} concentrations, as in eq 6a [and in more detail in Miller (1989)]. Similarly, the ratio of the total population of photosystem II centers to the subpopulation with Ca^{2+} bound in the Ca^{2+}-binding site is K_2.

$$K_1 = \frac{[P_{TOT}]}{[PMn_z] + [Ca_yPMn_z] + [Mn_aPMn_z]} = \left(1 + \frac{K_{Mn}}{[Mn^{2+}]^z}\left(1 + \frac{[Ca^{2+}]^b}{K'_{Ca}}\right)\right) \quad (6a)$$

$$K_2 = \left(1 + \frac{K_{Ca}}{[Ca^{2+}]^y}\left(1 + \frac{[Mn^{2+}]^a}{K'_{Mn}}\right)\right) \quad (6b)$$

Thus, in the case in which Ca^{2+} as well as Mn^{2+} needs to be bound for Mn photoligation to occur, the effective rate constant of photoactivation is

$$\kappa = k_i + (k_l/K_1K_2) \quad (7)$$

Therefore, the major difference between the two different modes of Ca^{2+} participation in photoactivation is that if Ca^{2+} must be bound for photoactivation to occur, then the rate of photoactivation is expected to be stimulated by Ca^{2+} as well as Mn^{2+}, whereas if only the content of the Mn-binding site is important, the rate is not expected to be stimulated by Ca^{2+}. Furthermore, the rate of photoactivation is expected to increase with Mn^{2+} and then level off, instead of dropping with increasing high Mn^{2+} concentration as the yield does. Note that the two different modes of Ca^{2+} participation in photoactivation are much less easily distinguished on the basis of measurements of the yield of photoactivation alone.

Figure 3 shows that photoactivation follows the time dependence predicted by eq 4a. Fits of eq 4a to time courses yielded estimates of $[\text{CaPSII}]_{t=\infty}$, the yield of photoactivation, and κ, the effective rate constant of photoactivation, at a range of Ca^{2+} and Mn^{2+} concentrations. Figure 4 shows that the effective rate constant increases with Mn^{2+} concentration initially as does the yield, but that the effective rate constant drops only slightly, if at all, at Mn^{2+} concentrations that were

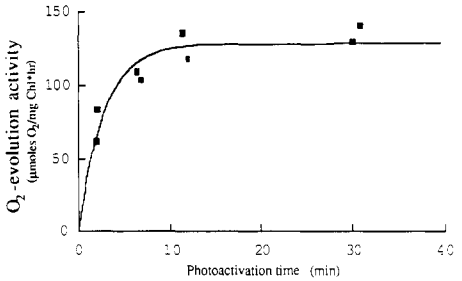

FIGURE 3: Time course of photoactivation. The O_2-evolution activity recovered is plotted as a function of time and accompanied by a fit of eq 4a. This time course was obtained in 15 mM Ca^{2+} and 2 mM Mn^{2+} and is accompanied by the best fit: O_2-evolution activity = [128 μmol of O_2/(mg of Chl·h)](1 − exp(−0.36 min^{-1} × time)).

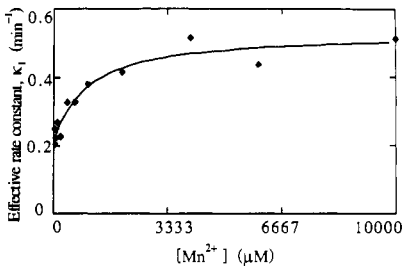

FIGURE 4: Dependence of the effective rate constant of photoactivation (κ) on Mn^{2+} concentration. The effective rate constant was obtained from fits of eq 4a to time courses of photoactivation in 50 mM Ca^{2+} and a range of Mn^{2+} concentrations. These rate constants are plotted as a function of the Mn^{2+} concentration and accompanied by a fit of eq 5: $\kappa = 0.215 + 0.315/(1 + 1000/[Mn^{2+}])$.

inhibitory to the yield of photoactivation (compare with Figure 2). Furthermore, when eq 5 was fit to the Mn^{2+} dependence of the effective rate constant, neither of the values of k_i nor k_l varied systematically with Ca^{2+} concentration. Thus, of the two equations for the effective rate constant of photoactivation (eq 5 and 7), eq 5 gives the best description of the Mn^{2+} and Ca^{2+} dependence. However, there did appear to be some stimulation of the effective rate constant by Ca^{2+} at the highest Mn^{2+} concentrations. The small stimulation of the effective rate constant of photoactivation by Ca^{2+} may be explained by a secondary effect of Ca^{2+}, such as stabilization of intermediates that are, nonetheless, not dependent on Ca^{2+} for their formation, as reported by Tamura and Cheniae (1989). Thus, we observe that Ca^{2+} stimulates primarily the yield of photoactivation and does not appear to be required in the rate-determining step(s) of photoactivation, whereas Mn^{2+} is required in the rate-determining step(s). Therefore, we conclude that photoactivation occurs in two stages, the rate-determining one of which depends primarily on Mn^{2+}. Of the two proposals for the participation of Ca^{2+}, this result is most consistent with that of Tamura and Cheniae (1987b) involving Ca^{2+}-independent Mn photoligation followed by Ca^{2+} binding.

Further support for photoactivation in two stages was obtained from experiments in which the Ca^{2+} or Mn^{2+} concentration was varied after Mn photoligation was complete. In these experiments, the O_2-evolution activity was observed to increase or decrease consistent with binding or displacement of Ca^{2+} from the Ca^{2+}-binding site. Furthermore, the same effects were observed with photosystem II membranes pretreated with 2 M NaCl to deplete the 17- and 23-kDa extrinsic polypeptides but not Mn. Therefore, the effect of Ca^{2+} or of excess Mn^{2+} can be ascribed to metal ion exchange at the Ca^{2+}-binding site alone, after assembly of the Mn complex is complete.

Photoinhibition, Photoinactivation, and the Yield of Photoactivation. The yields of photoactivation in photosystem II membranes do not approach 100% (Tamura & Cheniae, 1987a). Our optimal yield of 45% of the control O_2-evolution activity is fairly typical (Ananyev et al., 1988), though somewhat lower than that of Tamura and Cheniae (1987a). However, our data provide insights into the limitations on the yield of photoactivation.

Repeated cycles of photoactivation in various combinations of Mn^{2+} and Ca^{2+} concentrations, even interspersed with dark incubations and washes, indicate that the inability to undergo photoactivation is a stable feature of the photosystem II membranes that is acquired in the course of the first photoactivation cycle or is already present in the NH_2OH-treated photosystem II membranes. Specifically, one can attribute the less than quantitative yield of photoactivation to one of the following three types of damage to photosystem II: (1) damage to the photosystem II complex in the course of isolation or treatment with NH_2OH that does not impair O_2 evolution in the untreated sample but prevents photoactivation; (2) photoinhibition, which we define as a light-induced loss of primary electron transport; or (3) photoinactivation, which we define as a light-induced loss of photoactivation capability without a loss of primary electron transport. Assays of DPC-supported DCIP photoreduction allow the contribution of photoinhibition to be measured. Under conditions that produce a 40% yield of photoactivation, 25% of the photosystem II centers are photoinhibited. This leaves 35% of the centers unaccounted for. These centers might have been damaged before photoactivation, or they might have been photoinactivated during the photoactivation treatment.

Because $[P_{TOT}]_{t=0}$, the concentration of photosystem II centers competent to undergo photoactivation, is a parameter in the model for photoactivation (eq 4b), we can estimate the total competent population of photosystem II at the start of the photoactivation treatment. If F_0 is the initial fraction of the photosystem II centers that are competent to undergo photoactivation, and the yield of photoactivation is also stated as a fraction of the photosystem II centers, eq 4 and 5 yield

$$\text{fractional yield of photoactivation} = k_l F_0 / K_2(K_1 k_i + k_l) \quad (8)$$

where K_1 and K_2 (eq 6) are the equilibrium constants relating all photosystem II centers to those with the correct ion in the Mn- and Ca^{2+}-binding sites, respectively. The rate constants for photoinactivation (k_i) and Mn photoligation (k_l) can be estimated from the Mn^{2+} dependence of the effective rate constant of photoactivation (0.215 and 0.315 min^{-1}, respectively, in 50 mM Ca^{2+}, Figure 4) and used with the optimal yield of photoactivation (40%) corrected for 25% photoinhibition (0.40/0.75 = 0.53 at 50 mM Ca^{2+} and 1 mM Mn^{2+}) to give

$$0.114K_1K_2 + 0.167K_2 = 0.315F_0 \quad (9)$$

Substitution of the limiting value of 1 for K_1 and K_2 corresponds to assuming that the Mn^{2+} and Ca^{2+} concentrations that produce the optimal yield of photoactivation result in binding of only the correct ion in each binding site. This assumption gives the lower limit for F_0 of 0.89, so at least 90% of the photosystem II centers are competent to undergo photoactivation at the beginning of the photoactivation procedure. Therefore, we conclude that the process we have called photoinactivation does exist and significantly limits the yield of photoactivation, although no specific lesion was identified.

Equation 9 also enables us to calculate an upper limit for K_1 and K_2 under optimal conditions, using the limiting value of 1 for F_0. Assuming that $K_1 = K_2 = K^{1/2}$, this gives K = 1.1. The upper limit for either equilibrium constant is obtained

by using the minimum value for the other, giving $K_1 < 1.3$ and $K_2 < 1.1$. Thus, at least 80% (1/1.3) of the photosystem II sites have the correct ion complement in optimal Mn^{2+} and Ca^{2+} concentrations, and $K = K_1K_2$ approaches its theoretical minimum value of 1 under optimal conditions.

Extraction of Dissociation Constants for Mn^{2+} and Ca^{2+}. Mn photoligation followed by Ca^{2+} binding best accounts for the data in Figures 2–4. We now consider this model in more detail, to test its validity and to obtain dissociation constants and binding stoichiometries for Mn^{2+} and Ca^{2+} in photoactivation. The Mn^{2+} and Ca^{2+} dependences of photoactivation are embodied in the equilibrium constants K_1 and K_2 (see eq 6). To extract the Mn^{2+} and Ca^{2+} dependences, we must relate K_1 and K_2 to experimentally measurable quantities. These are the rate constant of photoactivation, κ (eq 5), and the yield of photoactivation, $[Ca\ PSII]_{t=\infty}$ (eq 3). Because we have determined that Ca^{2+} binds after assembly of the Mn complex, K_2 (eq 6b) is defined as $[P_{TOT}]/[CaPSII]$ and the product of K_1 and K_2 can be isolated by rearranging eq 4b to give

$$K = K_1K_2 = [P_{TOT}]_{t=0}k_1/[CaPSII]_{t=\infty}\kappa \qquad (10)$$

Because $[P_{TOT}]_{t=0}$ and k_1 are both constants, this expression indicates that the product of the effective rate constant, κ, and yield of photoactivation, $[CaPSII]_{t=\infty}$, at any combination of Ca^{2+} and Mn^{2+} concentrations should be inversely proportional to K. To evalute the equilibrium constant K, a value for the proportionality constant relating it to $\kappa\ [CaPSII]_{t=\infty}$ was required. This proportionality constant was obtained by assuming that the combination of Mn^{2+} and Ca^{2+} concentrations giving rise to the largest value for the product of the effective rate constant and yield of photoactivation (1 mM Mn^{2+} and 25 mM Ca^{2+}) optimized the content of both the Mn- and Ca^{2+}-binding sites, so that all photosystem II centers were assumed to bind Mn^{2+} in the Mn-binding site and Ca^{2+} in the Ca^{2+}-binding site under optimal conditions. This corresponds to assuming that K approaches its theoretical minimum value of 1 under optimal conditions when $[CaPSII]_{t=\infty}\kappa = ([CaPSII]_{t=\infty}\kappa)_{max}$. The validity of this assumption is supported by our calculations in the previous section and was tested at a number of stages in the analysis. Thus, $([CaPSII]_{t=\infty}\kappa)_{max}$ was used to replace $[P_{TOT}]_{t=0}k_1$ in eq 10, giving

$$K_{exp} = ([CaPSII]_{t=\infty}\kappa)_{max}/[CaPSII]_{t=\infty}\kappa \qquad (11)$$

where K_{exp} indicates the experimental value for K. Equation 11 was used to calculate an experimental value for K (K_{exp}) at a range of Mn^{2+} and Ca^{2+} concentrations. Then the dependence of K_{exp} on $[Mn^{2+}]$ and $[Ca^{2+}]$ was compared to the dependence predicted for K in

$$K = \left(1 + \frac{K_{Mn}}{[Mn^{2+}]^z}\left(1 + \frac{[Ca^{2+}]^b}{K'_{Ca}}\right)\right) \times \left(1 + \frac{K_{Ca}}{[Ca^{2+}]^y}\left(1 + \frac{[Mn^{2+}]^a}{K'_{Mn}}\right)\right) \qquad (12)$$

Manganese and Calcium Dependence of K. (a) Limiting Behavior at Low Manganese or Calcium Concentrations. In the presence of low Mn^{2+} concentrations, $[Mn^{2+}] < K'_{Mn}$, eq 12 reduces to

$$K = B + M(1/[Mn^{2+}])^z \qquad (13a)$$

where

$$B = 1 + (K_{Ca}/[Ca^{2+}]^y) \qquad (13b)$$

$$M = BK_{Mn}(1 + ([Ca^{2+}]^b/K'_{Ca})) \qquad (13c)$$

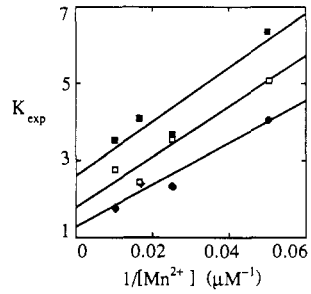

FIGURE 5: Comparison of the dependence of K_{exp} (the observed equilibrium between total photosystem II populations and populations with the correct ions bound) on $1/[Mn^{2+}]$, at three different Ca^{2+} concentrations. K_{exp} was calculated from eq 11. The lines resulting from fits of eq 13a to the data with $z = 1$ are shown along with the data. (■) 0.5 mM Ca^{2+} ($K_{exp} \approx 74\ \mu M \times [Mn^{2+}] + 2.5$); (□) 1.5 mM Ca^{2+} ($K_{exp} \approx 66\ \mu M \times [Mn^{2+}] + 1.8$); (◆) 15 mM Ca^{2+} ($K_{exp} \approx 55\ \mu M \times [Mn^{2+}] + 1.3$).

At a given Ca^{2+} concentration K is just a linear function of some integral power of $1/[Mn^{2+}]$. By comparison of plots of K_{exp} vs $1/[Mn^{2+}]$, $1/[Mn^{2+}]^2$, $1/[Mn^{2+}]^3$, and $1/[Mn^{2+}]^4$ the stoichiometry of Mn^{2+} binding in the Mn-binding site, z, was found to be 1, the power of $1/[Mn^{2+}]$ that resulted in the best straight line. Such plots were obtained at each of a range of Ca^{2+} concentrations and their Y intercepts (B) and slopes (M) tabulated. The Y intercepts and slopes are predicted to be simple functions of the Ca^{2+} concentration. Figure 5 shows a series of K_{exp} vs $1/[Mn^{2+}]$ plots and demonstrates the linearity of each, as well as the dependence of their slopes and intercepts on the Ca^{2+} concentration.

Analogous plots were obtained from data collected at subinhibitory Ca^{2+} concentrations ($[Ca^{2+}] \leq 25$ mM), and these were linear when K_{exp} was plotted against $(1/[Ca])^y$, with $y = 1$, with $[Mn^{2+}]$-dependent slopes and Y intercepts. That the data fit quite closely to straight lines in both these types of plots supports the validity of the model for photoactivation and the assumptions we have made.

M/B from seven K_{exp} vs $1/[Mn^{2+}]$ plots (such as those in Figure 5) was plotted as a function of $[Ca]^b$. A value of 1 for b gave a straight line in conformance with eq 13c. The Y intercept of this plot yielded a preliminary estimate for K_{Mn} of 33 μM (standard error of 1 μM), and the slope divided by the Y intercept yielded a preliminary estimate for K'_{Ca} of 53 mM (standard error of 5 mM).

The values of B derived from K_{exp} vs $1/[Mn^{2+}]$ plots were plotted against $1/[Ca]^y$. y was found to be 1 to obtain a straight line, as in the results discussed above. The slope gave a preliminary estimate of $K_{Ca} = 0.57$ mM (standard error of 0.07 mM) (eq 13b). The value of the Y intercept of this plot was 1.3, consistent with our assumption of $K_{min} = 1$, which predicts that it should be 1 (eq 13b).

(b) Limiting Behavior at High Manganese Concentrations. When $[Mn^{2+}] > K_{Mn}$, eq 12 reduces to

$$K = \left(1 + \frac{K_{Ca}}{[Ca^{2+}]^y}\right) + \frac{K_{Ca}}{[Ca^{2+}]^yK'_{Mn}}[Mn^{2+}]^a \qquad (14)$$

and

$$K = C + N[Mn^{2+}]^a \qquad (15a)$$

where

$$C = 1 + (K_{Ca}/[Ca^{2+}]^y) \qquad (15b)$$

$$N/(C - 1) = 1/K'_{Mn} \qquad (15c)$$

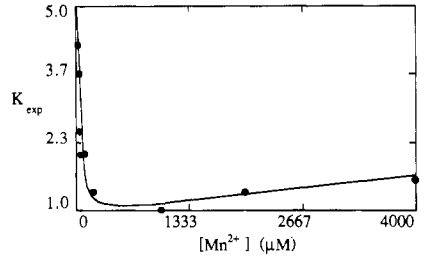

FIGURE 6: Dependence of K_{exp} (the observed equilibrium between total photosystem II populations and populations with the correct ions bound) on [Mn^{2+}] at 25 mM Ca^{2+}. K_{exp} was calculated from eq 11. The theoretical curve is derived from eq 12 with parameters obtained from the fits of eq 13a and 15a to the data obtained at low and high Mn^{2+} concentrations, respectively: $K = 0.00019\ \mu M^{-1} \times [Mn^{2+}] + 64\ \mu M/[Mn^{2+}] + 0.87$.

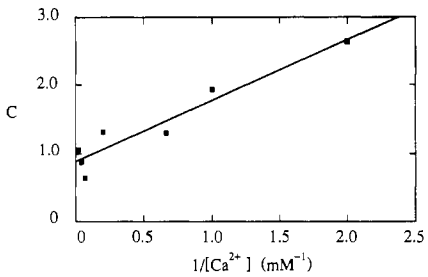

FIGURE 7: Y intercept obtained from plots of K_{exp} vs [Mn^{2+}] (C), plotted as a function of $1/[Ca^{2+}]$. K_{exp} values were calculated from eq 11 and fitted to eq 15a by using the dependence on [Mn^{2+}] at high Mn^{2+} concentrations. The resulting Y intercepts, C, for each Ca^{2+} concentration are shown here plotted against $1/[Ca^{2+}]$, along with the best fit of a straight line to these data ($C = 0.89\ mM/[Ca^{2+}] + 0.88$).

Thus, the model predicts that inhibition by Mn^{2+} should manifest itself as a linear dependence of K_{exp} on $[Mn^{2+}]^a$ at high Mn^{2+} concentrations. This is indeed observed for a binding stoichiometry of $a = 1$, as shown in Figure 6, which displays data from the full range of Mn^{2+} concentrations. Again, the predictions and the data agree extremely well.

Plots of K_{exp} as a function of [Mn^{2+}] at a series of Ca^{2+} concentrations and fits of eq 15a provide Y intercepts and slopes. Figure 7 shows that the Y intercepts (C) from K_{exp} vs [Mn^{2+}] plots increase linearly with $1/[Ca^{2+}]$ and that the Y intercept of the resulting line is 0.9, close to the value of 1 predicted by the model and our assumption of $K_{min} = 1$. This plot confirms a value for y of 1 and yields an estimate of K_{Ca} = 0.89 mM (standard error of 0.09 mM). Similarly, the combination $N/(C-1)$ of the slopes (N) and Y intercepts (C) from K_{exp} vs [Mn^{2+}] plots gives rise to an estimate of K'_{Mn} of 150 μM (standard error of 30 μM) (eq 15c).

Thus, we obtained preliminary estimates for all four dissociation constants. Furthermore, we find that photoactivation involves the equilibrium binding of *one* Mn^{2+} ion in the Mn-binding site for the step(s) that determine the rate and yield of photoactivation and then binding of *one* Ca^{2+} ion to generate O_2-evolution activity. In addition, binding of one incorrect ion at either site is inhibitory.

(*c*) *Behavior over the Whole Range of Manganese and Calcium Concentrations.* With z, y, a, and $b = 1$, eq 12 simplifies to

$$K = \left(1 + \frac{K_{Mn}}{[Mn^{2+}]}\left(1 + \frac{[Ca^{2+}]}{K'_{Ca}}\right)\right) \times \left(1 + \frac{K_{Ca}}{[Ca^{2+}]}\left(1 + \frac{[Mn^{2+}]}{K'_{Mn}}\right)\right) \quad (16)$$

Table II: Estimates of the Binding Stoichiometries and Dissociation Constants for Mn^{2+} and Ca^{2+} Binding to Photosystem II in Photoactivation[a]

K_{Mn} (μM), Mn^{2+} in the Mn site	K'_{Ca} (mM), Ca^{2+} in the Mn site	K_{Ca} (mM), Ca^{2+} in the Ca^{2+} site	K'_{Mn} (μM), Mn^{2+} in the Ca^{2+} site
	Dissociation Constants		
51 (5)	70 (40)	0.3 (0.1)	90 (45)
	Binding Stoichiometries		
$z = 1$	$b = 1$	$y = 1$	$a = 1$

[a] The estimates shown for the dissociation constants were obtained from a fit of eq 16 to the entire data set. The standard errors are given in parentheses.

and we can neglect the possibilities of Ca^{2+} and Mn^{2+} binding together in a binding site or cooperative binding. To obtain the best estimate for the dissociation constants, the average preliminary estimates from limited ranges of concentrations (above) were used as starting values in a fit of eq 16 to data from the full range of Mn^{2+} and Ca^{2+} concentrations. This fit resulted in somewhat lower estimates for K_{Ca} and K'_{Mn} than had been obtained from the linear fits. The refined estimates for the dissociation constants are listed in Table II.

The minimum value of K is probably slightly larger than 1, although our calculations in the section on photoinactivation indicate that $K \leq 1.3$ under optimal conditions. One indication that the minimum value of K is slightly larger than 1 is that, at the highest Ca^{2+} concentrations, the Mn^{2+} concentration at which the effective rate constant of photoactivation reached its maximum was higher than the optimum Mn^{2+} concentration for the yield of photoactivation. This suggests that high Ca^{2+} concentrations result in some Ca^{2+} binding in the Mn-binding site, even at the optimal Mn^{2+} concentration with respect to the yield of photoactivation. Thus, K'_{Ca} may be somewhat lower than calculated (Table II), in agreement with a K_{min} greater than 1. Nonetheless, the dissociation constants did not change by more than the standard errors in Table II when K_{min} was allowed to vary from the assumed value of 1.

Discussion

Two-Stage Model of Photoactivation. We find that photoactivation proceeds in two stages with different Ca^{2+} dependences, in agreement with the conclusions of Tamura and Cheniae (1987b). The two stages are Mn photoligation, which does not require Ca^{2+}, followed by rapid Ca^{2+} binding [also, Tamura and Cheniae (1989)]. We have developed a mathematical model for this mode of Mn^{2+} and Ca^{2+} participation in photoactivation. The overall agreement between our data and this model is excellent, indicating that any errors stemming from our assumptions are not serious and that the two-stage model provides a useful and accurate description of the Mn^{2+} and Ca^{2+} dependences of photoactivation. This model also provides the means for determining the dissociation constants and binding stoichiometries for Mn^{2+} and Ca^{2+} in both the Mn- and Ca^{2+}-binding sites in the rate-determining step(s) of photoactivation. This information provides new insight into the mechanism of photoactivation, which we discuss below.

Our results contradict those of Ono and Inoue (1983), who concluded that Ca^{2+} is required in the rate-determining step(s) of photoactivation. These authors assumed that the rate of photoactivation was proportional to the water-oxidation activity recovered after 8 min, but did not show the effects of Ca^{2+} and Mn^{2+} on the final yield of photoactivation. Because a single measurement of the water-oxidation activity will reflect the equilibrium at the Ca^{2+}-binding site as well as the rate of

Scheme I: Elementary Steps Involved in Production of the First Stable Intermediate of Photoactivation[a]

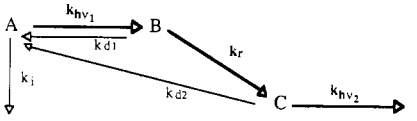

[a] B and C are unstable intermediates. A is an unactivated photosystem II center. The first stable intermediate is formed upon photooxidation of C. k_i is the rate constant for photoinactivation, $k_{h\nu 1}$ and $k_{h\nu 2}$ are the rates of the photochemical steps, k_r is the rearrangement rate of B, and k_{d1} and k_{d2} are the decay rates of B and C, respectively.

photoactivation, it is, indeed, expected that a single measurement will suggest stimulation by both Ca^{2+} and Mn^{2+}. The two-stage model predicts that the effective rate constant of photoactivation would be affected primarily by the Mn^{2+} concentration in the experiments of Ono and Inoue (1983) but that the Ca^{2+} concentration would affect the fraction of reconstituted photosystem II centers that expressed water-oxidation activity. This, we believe, is the principal source of the Ca^{2+} dependence observed by Ono and Inoue (1983), rather than a large Ca^{2+} dependence of the effective rate of photoactivation itself.

Dissociation Constants for Manganese and Calcium. The two-stage model for photoactivation provides dissociation constants for Mn^{2+} and Ca^{2+} that compare well with those in the literature. Of the two Ca^{2+} ions bound per photosystem II when maximum O_2-evolution activity is expressed (Cammarata & Cheniae, 1987; Katoh et al., 1987; Ono & Inoue, 1988), the dissociation constants we have obtained probably apply to the weaker Ca^{2+}-binding site, which is expected to be in equilibrium with the medium under our conditions of dilution, ionic strength, and illumination (Dekker et al., 1984; Ghanotakis et al., 1984a; Ono & Inoue, 1986; Miyao & Murata, 1986). Ghanotakis et al. (1984b) have reported a dissociation constant for Ca^{2+} of 0.5 mM, close to our estimate of 0.3 mM. Mn^{2+} binds to the Ca^{2+}-binding site with strength comparable to that of Ca^{2+} binding, in agreement with Ono and Inoue (1983). This is not unexpected; the binding of Mn^{2+} is generally similar in strength or a little stronger than that of Ca^{2+} to the carboxylate ligands usually involved in Ca^{2+} ligation by proteins (Sigel & McCormick, 1970).

Our estimate of K_{Mn} (51 μM) compares very well with the value of 40 μM obtained by Ono and Inoue (1983). Klimov et al. (1982) and Hsu et al. (1987), however, have reported dissociation constants of less than 1 μM for Mn^{2+} at the Mn-binding site of Mn-depleted photosystem II membranes from studies of Mn^{2+}-supported DCIP photoreduction or the competitive inhibition of DPC-supported DCIP photoreduction by Mn^{2+}. In both cases, the measurements involve electron donation by Mn^{2+}. Once oxidized to Mn^{3+}, Mn would be much more tightly bound, so the dissociation constant measured in those experiments could reflect an on-rate for Mn^{2+} and a very slow off-rate for Mn^{3+}. Thus, the values of Hsu et al. (1987) and Klimov et al. (1982) are more likely to represent an *effective* dissociation constant for Mn that is photooxidized or the concentration at which there were stoichiometric amounts of Mn available to mediate electron donation to photosystem II (Velthuys, 1983) rather than a concentration at which Mn^{2+} was bound in half the sites.

The dissociation constants of Mn^{2+} and Ca^{2+} (Table II) and the equations derived from the two-stage model for photoactivation can be used to calculate the optimal Mn^{2+} and Ca^{2+} concentrations for photoactivation and the ion content of the Ca^{2+}-binding site in O_2-evolving photosystem II membranes at a given combination of Mn^{2+} and Ca^{2+} concentrations. When the derivative of eq 12 with respect to $[Ca^{2+}]$ is equated to zero, the resulting expression can be solved for $[Ca^{2+}] = [Ca^{2+}]_{optimum}$.

$$[Ca^{2+}]_{optimum} = \left[K_{Ca}K'_{Ca}\left(1 + \frac{[Mn^{2+}]}{K_{Mn}}\right)\left(1 + \frac{[Mn^{2+}]}{K'_{Mn}}\right)\right]^{1/2} \quad (17a)$$

Similarly

$$[Mn^{2+}]_{optimum} = \left[K_{Mn}K'_{Mn}\left(1 + \frac{[Ca^{2+}]}{K'_{Ca}}\right)\left(1 + \frac{[Ca^{2+}]}{K_{Ca}}\right)\right]^{1/2} \quad (17b)$$

Our results indicate that it is possible to favor Mn^{2+} binding in the Mn-binding site and Ca^{2+} binding in the Ca^{2+}-binding site. However, slightly better final yields of photoactivation may be obtained by using slightly supraoptimal Mn^{2+} concentrations and following Mn photoligation with an incubation in high Ca^{2+} concentration buffer, under photoactivation conditions, to displace any Mn^{2+} in the Ca^{2+}-binding site.

Photoinactivation, which irreversibly inactivates photosystem II with respect to photoactivation, without inhibiting DPC-supported DCIP photoreduction, was found to be a significant limitation on high yields of photoactivation. Photoinactivation could be due to photochemical damage to the Mn-binding site or photooxidation of inappropriately bound Mn^{2+}. This would not necessarily reduce the rate of primary electron transport or the observed rate of DPC-supported DCIP photoreduction, which is limited by the rate of electron transfer to DCIP on the electron-acceptor side of photosystem II. Further efforts to optimize photoactivation yields should be directed at decreasing the tolls of photoinactivation and photoinhibition.

Mechanism of Photoactivation. The four Mn ions in the active Mn complex are in a higher average oxidation state than Mn^{2+}. Thus, the photochemical reactions of photoactivation leading to Mn photoligation must result in oxidation of Mn^{2+}. Previous studies of photoactivation in flashing light indicate that the first stable intermediate is formed following two photochemical steps separated by a light-independent step (Cheniae & Martin, 1971; Ono & Inoue, 1987; Ananyev et al., 1988). The two photochemical events of photoactivation have been proposed to be photooxidation of Mn^{2+} (Ono & Inoue, 1987; Tamura & Cheniae, 1989).

Kinetic analyses provide further information on the rate-determining steps of photoactivation. Our results show that one Mn^{2+} is involved in the rate-determining step(s) of photoactivation. In addition, the rate of photoactivation depends on illumination intensity (Cheniae & Martin, 1971); therefore, the rate-determining step(s) involve photochemistry. However, to interpret these results in terms of the mechanism of photoactivation, the invididual steps of photoactivation must be identified.

The results of previous studies using flashing light (Cheniae & Martin, 1971; Ono & Inoue, 1987; Ananyev et al., 1988) provide information on the intermediates before the first stable intermediate is formed, as shown in Scheme I. The photochemical events themselves, such as photooxidation of bound Mn^{2+}, are intrinsically rapid [for example, Hoganson et al. (1988)]. However, the initial intermediates are unstable (Ono & Inoue, 1987; Tamura & Cheniae, 1989), consistent with the low quantum yield of Mn photoligation (Cheniae & Martin, 1971). Each intermediate may form and decay many times before advancing, and the observed rate of photoactivation is expected to be much lower than the slowest individual

step. The identity of the rate-determining (and yield-determining) step(s) depends on which intermediate is least stable and most likely to be formed repeatedly.

Because optimization of the yield of photoactivation corresponds to optimizing the branching ratio between it and photoinactivatory processes, the light intensity that produces the optimal yield should be that in which the efficiency of photoactivation on a per-quantum basis is optimized. In a mechanistic sense, this corresponds to ensuring that one of the two photochemical steps in Scheme I is light-saturated, but not both. As long as neither reaction is saturated, the efficiency of photoactivation increases with increasing illumination intensity, but once one is saturated, the rate of photoactivation is a linear function of illumination intensity and the efficiency is constant and maximal (Cheniae & Martin, 1971). Thus, the more difficult photochemical step to saturate determines the rate and yield of photoactivation.

Depending on which photochemical step is saturated, either (1) maximum amounts of B are available for the light-independent step, if A → B is light-saturated, or (2) all of C formed is stabilized, if photooxidation of C is light-saturated (Scheme I). In either case the observed rate of photoactivation should be equal to the product of the rate of the light-independent step (B → C) and the fractional success of the photochemical step that is not saturated. We favor case 1 because a 2-fold increase in the rate of decay of C observed in the presence of reductants was accompanied by a 2-fold decrease in the yield of photoactivation (Ono & Inoue, 1987) (implying that the rate of stabilization of C is relatively slow, consistent with the low quantum yield). This interpretation is supported by the results of experiments in which photoactivation was measured after a series of flashes. If first-order kinetics are used to describe the various steps of photoactivation shown in Scheme I, after a single flash

$$[B] = (k_{h\nu 1}/(k_{h\nu 1} - \kappa_B))[A]_{t=0}(e^{-\kappa_B t} - e^{-k_{h\nu 1} t}) \quad (18)$$

where $\kappa_B = k_{d1} + k_r$ is the rate at which B is consumed, k_{d1} is the decay rate of B, k_r is the rearrangement rate of light-independent conversion of B to C, $k_{h\nu 1}$ is the rate of photochemical formation of B from A, and $[A]_{t=0}$ is the concentration of A present before the flash. Because κ_B must be significantly smaller than $k_{h\nu 1}$ for photoactivation to succeed, the exponential term containing $k_{h\nu 1}$ can be ignored. Then it follows that

$$[C] = \frac{k_r}{(\kappa_B - k_{d2})} \frac{k_{h\nu 1}}{(k_{h\nu 1} - \kappa_B)} [A]_{t=0}(e^{-k_{d2} t} - e^{-\kappa_B t}) \quad (19)$$

where k_{d2} is the decay rate of C. Equation 19 describes the amount of C eligible for photochemical stabilization a time interval t after a flash of light. It is analogous to eq 2 in Tamura and Cheniae (1987a), but allows for the decay not only of the second intermediate, C, but also of the first, B.

When the yield of photoactivation after 200 flashes is plotted as a function of the spacing between flashes, the profile is interpreted to reflect the concentration of C present as a function of time since a flash (Ono & Inoue, 1987). The initial rise in yield with increasing (short) flash spacing provides an estimate of the half-time of formation of C; the half-time of C's decay is obtained from the decrease in yield at long flash spacings. Reductants decrease the yield of photoactivation, especially when it is performed in widely spaced flashes (Tamura & Cheniae, 1987b). However, Ono and Inoue (1987) observed that the rate of formation of C was not significantly affected. Because C is formed with an effective rate constant that also includes the decay rate of B, this result indicates that the stability of B did not change or that it is not a limiting factor ($k_{d1} < k_r$) and $\kappa_B \approx k_r$. The former is somewhat less likely because B is an oxidized species, but in either case it is apparent that formation of B from A is not a limiting step of photoactivation and does not determine the yield (and rate) of photoactivation. The 2-fold decrease in the lifetime of C observed in the presence of reductants would shift the time after one flash at which the maximum amount of C is present to earlier in the course of formation of C. The combination of hastened decay and earlier optimum could explain the 2-fold reduction in the yield of photoactivation observed to accompany the reduced stability of C. These results indicate that decay of C in competition with photochemical stabilization of C contributes to the yield (and rate) of photoactivation. Therefore, we identify the conversion of B to C and subsequent stabilization of C as the rate-determining steps of photoactivation.

The submicromolar effective dissociation constants reported for Mn in connection with Mn^{2+} photooxidation (Hsu et al., 1987; Klimov et al., 1982) are consistent with assignment of A → B to binding and photooxidation Mn^{2+} (Tamura & Cheniae, 1989) and our conclusion that B is present in the steady-state during illumination. It follows that Mn would always be bound in this first step at the Mn^{2+} concentrations necessary for substantial photoactivation yields, so that the first step would not contribute any Mn^{2+} dependence to the rate of photoactivation.

The conversion of B to C could involve binding of Mn^{2+}. This possibility is supported by the fact that Mn is the species photooxidized by the photochemical steps of photoactivation (Miller, 1989; Tanura & Cheniae, 1989), but only one Mn ion is bound after the first photochemical event (Miller, 1989). Thus, acquisition of another Mn^{2+} by intermediate B would prepare the photosystem II center for the second photochemical event. On the basis of the Mn^{2+} dependence of photoactivation, we propose that B is converted to C by ligation of one Mn^{2+} ion in preparation for photooxidation, and our dissociation constant applies to binding of Mn^{2+} to B. Therefore, assignment of the rate-determining steps to formation and photostabilization of C is consistent with the dependence of the rate of photoactivation on illumination intensity, the binding of a single Mn^{2+} ion in the rate-determining step, and the slowness of photoactivation relative to the rate of Mn^{2+} photooxidation.

A mechanism of photoactivation that incorporates these results and conclusions is shown in Scheme II. Although a mechanism of photoactivation similar to that shown in Scheme II has been proposed before (Tamura & Cheniae, 1987a), we have obtained the first direct evidence on the nature of the second step in photoactivation. Intermediate B in Scheme I has been proposed to contain Mn^{3+} (Ono & Inoue, 1987; Tamura & Cheniae, 1989), and direct evidence for this has been reported (Miller, 1989). The binding of one Mn^{2+} that we have characterized in this paper then would produce $Mn^{2+}Mn^{3+}$ (intermediate C). Subsequent photooxidation would result in production of the $Mn^{3+}Mn^{3+}$ intermediate inferred by analogy with the product of partial Mn depletion (Cole et al., 1987). Upon acquisition of two more Mn^{2+} ions to form a tetranuclear complex, the nascent Mn complex becomes resistant to EDTA extraction in this model. This is consistent with our observed retention of four Mn ions per photoactivated photosystem II center and none by the other centers after they were washed with EDTA (Table I). Successive photochemical events would then result in formation of the S states of the Mn complex, at least one of which binds the Ca^{2+} essential for O_2-evolution activity.

Scheme II: Proposed Mechanism of Photoactivation[a]

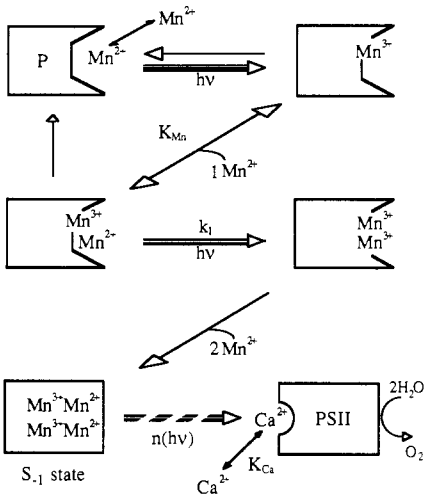

[a] P denotes an unactivated photosystem II center; PSII denotes a photosystem II center with the Mn complex assembled.

It is tempting to equate the least oxidized stable tetranuclear state formed in photoactivation, $Mn^{3+}{}_2Mn^{2+}{}_2$, with the most reduced stable state of the Mn complex, S_{-1} [formed upon reaction of dark-adapted photosystem II membranes with 0.2 mM NH_2OH in the dark (Beck & Brudvig, 1987)]. This leads to assignment of the S_2 state to $Mn^{3+}{}_3Mn^{4+}$, which is consistent with the EPR signals produced by the S_2 state of the Mn complex, EXAFS measurements, and ultraviolet absorption changes during S-state advancement [reviewed in Brudvig and Crabtree (1989)].

Registry No. Mn, 7439-96-5; Ca, 7440-70-2; O_2, 7782-44-7.

REFERENCES

Ananyev, G. M., Shafiev, M. A., Isaenko, T. V., & Klimov, V. V. (1988) *Biofizika 33*, 265.

Arnon, D. I. (1949) *Plant Physiol. 24*, 1.

Babcock, G. T. (1987) *New Comprehensive Biochemistry: Photosynthesis* (Amesz, J., Ed.) p 125, Elsevier, Amsterdam.

Babcock, G. T., Ghanotakis, D. F., Ke, B., & Diner, B. A. (1983) *Biochim. Biophys. Acta 723*, 276.

Beck, W. F., & Brudvig, G. W. (1987) *Biochemistry 26*, 8285.

Beck, W. F., de Paula, J. C., & Brudvig, G. W. (1985) *Biochemistry 24*, 3035.

Becker, D. W., Callahan, F. E., & Cheniae, G. M. (1985) *FEBS Lett. 192*, 209.

Berthold, D. A., Babcock, G. T., & Yocum, C. F. (1981) *FEBS Lett. 134*, 231.

Brudvig, G. W., & Crabtree, R. H. (1989) *Prog. Inorg. Chem. 37*, 99.

Callahan, F. E., & Cheniae, G. M. (1985) *Plant Physiol. 79*, 777.

Callahan, F. E., Becker, D. W., & Cheniae, G. M. (1986) *Plant Physiol. 82*, 261.

Cammarata, K. V., & Cheniae, G. M. (1987) *Plant Physiol. 84*, 587.

Cheniae, G. M., & Martin, I. F. (1966) *Brookhaven Symp. Biol. 19*, 406.

Cheniae, G. M., & Martin, I. F. (1967) *Biochem. Biophys. Res. Commun. 28*, 89.

Cheniae, G. M., & Martin, I. F. (1971) *Biochim. Biophys. Acta 253*, 167.

Cole, J. L., Yachandra, V. K., McDermott, A. E., Guiles, R. D., Britt, R. D., Dexheimer, S. L., Sauer, K., & Klein, M. P. (1987) *Biochemistry 26*, 5967.

Dekker, J. P., Ghanotakis, D. F., Plijter, J. J., Van Gorkom, H. J., & Babcock, G. T. (1984) *Biochim. Biophys. Acta 767*, 515.

de Paula, J. C., Innes, J. B., & Brudvig, G. W. (1985) *Biochemistry 24*, 8114.

de Paula, J. C., Li, P. M., Miller, A.-F., Wu, B. W., & Brudvig, G. W. (1986) *Biochemistry 25*, 6487.

Eyster, C., Brown, T. E., Tanner, H. A., & Hood, S. L. (1958) *Plant Physiol. 33*, 235.

Gerhardt, B., & Weissner, W. (1967) *Biochem. Biophys. Res. Commun. 28*, 958.

Ghanotakis, D. F., Babcock, G. T., & Yocum, C. F. (1984a) *FEBS Lett. 167*, 127.

Ghanotakis, D., Topper, J. N., Babcock, G. T., & Yocum, C. (1984b) *FEBS Lett. 170*, 169.

Hoganson, C. W., Babcock, G. T., & Yocum, C. F. (1988) *Biophys. J. 53*, 616a.

Homan, P. H. (1967) *Plant Physiol. 42*, 997.

Hsu, B. D., Lee, J. Y., & Pan, R.-L. (1987) *Biochim. Biophys. Acta 890*, 89.

Jones, L. W., & Kok, B. (1966) *Plant Physiol. 41*, 1037.

Katoh, S., Satoh, K., Ohno, T., Chen, J.-R., & Kasino, K. (1987) *Progress in Photosynthesis Research* (Biggins, J., Ed.) Vol. 1, pp 625, Martinus Nijhoff, Dordrecht, The Netherlands.

Klimov, V. V., Allakhverdiev, S. I., Shuvalov, V. A., & Krasnovsky, A. A. (1982) *FEBS Lett. 148*, 307.

Miller, A.-F. (1989) Ph.D. Thesis, Yale University.

Miyao, M., & Murata, N. (1986) *Photosynth. Res. 10*, 489.

Ono, T., & Inoue, Y. (1982) *Plant Physiol. 69*, 1418.

Ono, T., & Inoue, Y. (1983) *Biochim. Biophys. Acta 723*, 191.

Ono, T., & Inoue, Y. (1986) *Biochim. Biophys. Acta 850*, 380.

Ono, T., & Inoue, Y. (1987) *Plant Cell Physiol. 28*, 1293.

Ono, T., & Inoue, Y. (1988) *FEBS Lett. 227*, 147.

Pistorius, E. K., & Schmid, G. H. (1984) *FEBS Lett. 171*, 173.

Sigel, H., & McCormick, D. B. (1970) *Acc. Chem. Res. 3*, 201.

Tamura, N., & Cheniae, G. M. (1986) *FEBS Lett. 200*, 231.

Tamura, N., & Cheniae, G. M. (1987a) *Biochim. Biophys. Acta 890*, 179.

Tamura, N., & Cheniae, G. M. (1987b) in *Progress in Photosynthesis Research* (Biggins, J., Ed.) Vol 1, pp 621, Martinus Nijhoff, Dordrecht, The Netherlands.

Tamura, N., & Cheniae, G. M. (1989) *Plant Physiol.* (in press).

Thompson, L. K., & Brudvig, G. W. (1988) *Biochemistry 27*, 6653.

Velthuys, B. (1983) in *The Oxygen Evolving System of Photosynthesis* (Inoue, Y., Crofts, A. R., Govindjee, Murata, N., Renger, G., & Satoh, K., Eds.) p 83, Academic Press, New York.

Yamashita, T., & Tomita, G. (1971) *Plant Cell Physiol. 12*, 117.

Yamashita, T., & Tomita, G. (1976) *Plant Cell Physiol. 17*, 571.

Yocum, C. F., Yerkes, C. T., Blankenship, R. E., Sharp, R. R., & Babcock, G. T. (1981) *Proc. Natl. Acad. Sci. U.S.A. 78*, 7507.